arXiv:2111.11230v3 [cond-mat.stat-mech] 25 Feb 2022

Near universal values of social inequality indices in self-organized critical models

S. S. Manna[a,1], Soumyajyoti Biswas[b,2], Bikas K. Chakrabarti[c,a,d,3]

[a] *Satyendra Nath Bose National Centre for Basic Sciences, Block-JD, Sector-III, Salt Lake, Kolkata-700106, India*
[b] *Department of Physics, SRM University - AP, Andhra Pradesh - 522502, India*
[c] *Saha Institute of Nuclear Physics, Kolkata - 700064, India*
[d] *Economic Research Unit, Indian Statistical Institute, Kolkata 700026, India*

Abstract

We have studied few social inequality measures associated with the sub-critical dynamical features (measured in terms of the avalanche size distributions) of four self-organized critical models while the corresponding systems approach their respective stationary critical states. It has been observed that these inequality measures (specifically the Gini and Kolkata indices) exhibit nearly universal values though the models studied here are widely different, namely the Bak-Tang-Wiesenfeld sandpile, the Manna sandpile and the quenched Edwards-Wilkinson interface, and the fiber bundle interface. These observations suggest that the self-organized critical systems have broad similarity in terms of these inequality measures. A comparison with similar earlier observations in the data of socio-economic systems with unrestricted competitions suggest the emergent inequality as a result of the possible proximity to the self-organized critical states.

1. Introduction

Unequal distributions of resources (for example income or wealth) among the population are ubiquitous. Social scientists, economists in particular, traditionally quantify such inequalities in distributions using some inequality indices, defined through the Lorenz function $L(p)$ [1]. After ordering the population from the poorest to the richest, the Lorenz function $L(p)$ is given by the cumulative wealth fraction possessed by the p fraction of the population staring from the poorest: $L(0) = 0$ and $L(1) = 1$ (see Fig. 1). If everyone had equal share of wealth, $L(p) = p$ would be linear (called the equality line) and the old and still most popular inequality index, namely the Gini (g) index [2] is given by the ratio of the area between the equality line and the Lorenz curve and the entire area (1/2) below the equality line. As such, $g = 0$ corresponds to perfect equality and $g = 1$ corresponds to extreme inequality. Another recently introduced inequality index, namely the Kolkata (k) index [3], can be defined as the nontrivial fixed point of the complementary Lorenz function $\tilde{L}(p) \equiv 1 - L(p)$: $\tilde{L}(k) = k$. It says, $(1 - k)$ fraction of people possess k fraction of wealth ($k = 1/2$ corresponds to perfect equality and $k = 1$ corresponds to extreme inequality). As such, k index quantifies and generalizes (see e.g., [4]) the (more than a) century old 80-20 law ($k = 0.8$) of Pareto [5]. Extensive analysis of social data (see e.g., [6, 7]) indicated that in extremely competitive situations, the indices k and g equals each other in magnitude and becomes about 0.87.

[1] subhrangshu.manna@gmail.com
[2] soumyajyoti.b@srmap.edu.in
[3] bikask.chakrabarti@saha.ac.in

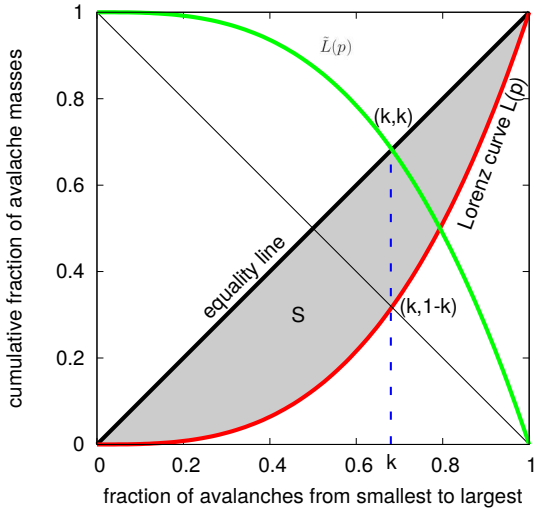


Figure 1: The Lorenz curve $L(p)$ (shown in red) and complementary Lorenz curve $\tilde{L}(p)$ (shown in green) used to calculate the inequality indices Gini ($g = 2S$) and Kolkata (given by the fixed point $k = \tilde{L}(k)$) are shown. For the systems considered here, the horizontal axis represents the fraction of avalanches, when all avalanches are arranged from lowest to the highest size. The vertical axis is the fraction of the cumulative mass of these avalanches.

In physics, starting from kinetic theory models to that of the phase transitions, unequal distributions of quantities like energy, domain sizes, avalanche sizes, etc. are widely observed. In the renormalization group theory, we look for the self-similar limit (fixed point) of the generators of such distributions, where inequalities become extreme and one dominant (fractal) cluster emerges and eventually brings about the phase transition. Because of this, while the fractal dimensions (exponents) become universal, the fixed point itself (where only a single dominant cluster emerges) do not become so. Social statistics, on the other hand, look for the fixed point of the inequality distribution, where the larger inequalities set in, but they appear with commensurately large frequencies (or numbers). This some times (most likely due to self-organization induced by extreme competition) leads to some universal value of the inequality indices (fixed points) like those of g or k indices discussed above. Indeed, a recent study [8] of the k index near the breaking point of the bundle in the Fiber Bundle model, showed that k attains a stable value of about 0.62 (or inverse of the Golden Ratio). This, however, is not a self-organized critical system and the terminal values of g and k are not equal.

In this work, we consider four models where self-organized criticality (SOC) was well investigated before. Specifically, we study the Bak-Tang-Wiesenfeld (BTW) [9] and Manna [10] sandpile models and the driven Edwards-Wilkinson (EW) [11] and the centrally loaded fiber bundle [12] interface models. In each of these models, a slow external drive brings the activity rate (toppling rate of the sand grains, or the velocity of the interface) from zero to a higher value, where it saturates upon reaching the SOC state. On the path to reach the SOC state, the avalanches or the cluster of activities are of unequal sizes. We measure the inequality indices (g and k) of the avalanche sizes for these models along their paths towards the respective SOC states. We find that in all these four SOC models the two indices (g and k) become equal (about 0.87) where the SOC sets in, even though the models represent very different universality classes.

In view of the fact that the socio-economic systems mentioned before have long been conjectured to operate near the SOC state, and the inequality analysis of those systems reveal $g_c = k_c \approx 0.87$, there are two main implications of our observations in the SOC models here. First, it stands as

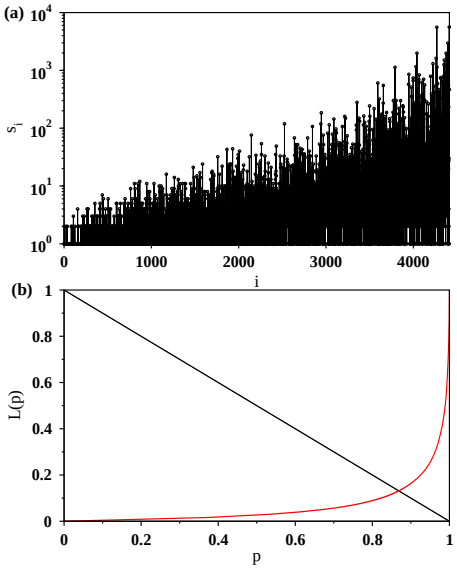


Figure 2: A plot for the BTW sandpile model on the square lattice of size $L = 128$ in the subcritical phase starting from an empty lattice. (a) The non-zero avalanche sizes s_i have been plotted against their serial number i. (b) The Lorenz function (cumulative avalanche size) $L(p)$ has been plotted along the y-axis against the fraction p of non-zero avalanches ordered in the sequence of increasing sizes.

the quantitative evidence of social systems with unrestricted competitions operating near the SOC state. Second, the time evolution of g and k can help in estimating the 'distance' from the SOC state, where such systems reach a steady state.

2. Inequality measures in the BTW and Manna sandpile models

In this section, we first describe the dynamics of the BTW [9] and Manna [10] sandpile models. In the following sub-section we describe the method used for the estimation of inequality measures and report the results obtained for these models.

2.1. Dynamics of the BTW sandpile model

On a square lattice of size $L \times L$ sand grains are dropped one at a time at the randomly selected lattice sites with coordinates (i, j). Let us denote the number of sand grains at a site by $h(i, j)$. Therefore, the addition of a grain implies the unit increase of the height of the sand column:

$$h(i, j) \rightarrow h(i, j) + 1.$$

A threshold value $h_c = 4$ for the height of the sand column has been pre-assigned for its stability which is assumed to be the same for all sites. If the height of a sand column becomes equal to, or larger than the threshold height i.e., $h(i, j) \geq h_c$, that sand column becomes unstable and it topples immediately. In a toppling, the sand column looses 4 grains which are then distributed to the neighboring sites uniformly:

$$h(i, j) \rightarrow h(i, j) - 4$$
$$h(i \pm 1, j \pm 1) \rightarrow h(i \pm 1, j \pm 1) + 1.$$

On receiving sand grains, some of the neighboring sites may topple again which distribute grains leading to further toppling. In this way, a cascade of sand column toppling takes place as a domino

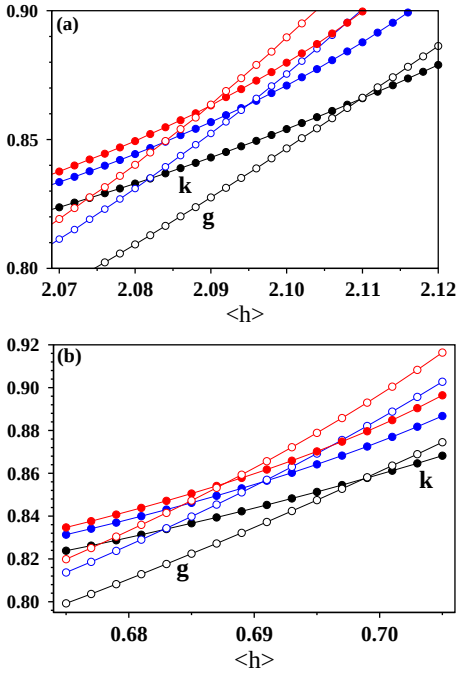


Figure 3: (a) BTW sandpile model: Plot of the Kolkata index $k(\langle h\rangle, L)$ (filled circles) and the Gini coefficient $g(\langle h\rangle, L)$ (empty circles) against the terminating average sandpile height $\langle h\rangle$ for $L = 128$ (black), 256 (blue) and 512 (red). For each lattice size L these two curves meet at a point whose y coordinate is $k_c(L) = g_c(L)$ and the corresponding x coordinate is the average height $\langle h_c(L)\rangle$. The estimated values are: $k_c(L) = g_c(L) = 0.8657, 0.8634, 0.8627$ and $\langle h_c(L)\rangle = 2.110, 2.095, 2.090$ for $L = 128$, 256, and 512 respectively. (b) Manna sandpile model: Same quantities have been plotted for the same lattice sizes using the same symbols. The estimated values are: $k_c(L) = g_c(L) = 0.8573, 0.8558, 0.8555$ and $\langle h_c(L)\rangle = 0.6987, 0.6906, 0.6877$ for $L = 128$, 256, and 512 respectively.

effect. The sequence of topplings is referred as an 'avalanche' which terminates only when none of the lattice sites remain unstable. The boundary of the lattice is assumed to be open on all four sides. In the case of toppling at a boundary site, one or two sand grains leave the system and never come back. A typical measure of the strength of the avalanche is the total number of toppings in an avalanche and is referred as the 'size' s of the avalanche. Usually, one starts from an empty lattice and adds sand grains one by one at randomly selected sites. Therefore, the sizes of the avalanches in the early stage are quite small which gradually become larger. Eventually, a stationary state is reached when the outflow rate sand mass becomes equal to the inflow rate on the average. In the stationary state of an infinitely large systems $L \to \infty$ the avalanche sizes are expected to be of 'all' length and time scales and their probability distributions are characterized by the power law decays, a signature of the self-organized critical state. However, for the finite size systems the avalanche sizes are limited to some L dependent cut-off values: $s_c(L) \sim L^{\beta}$. The average height $\langle h\rangle$ per site of the sand column initially grows but eventually reaches a steady value $\langle h(L)\rangle$ in the stationary state. For the infinitely large system $\langle h\rangle = 17/8$ is an analytically estimated value [13].

2.2. Dynamics of the Manna sandpile model

This is a variant of the BTW sandpile model where the threshold height for stability is assumed to be $h_c = 2$. When a sand column topples, it looses only 2 grains which are then distributed to the

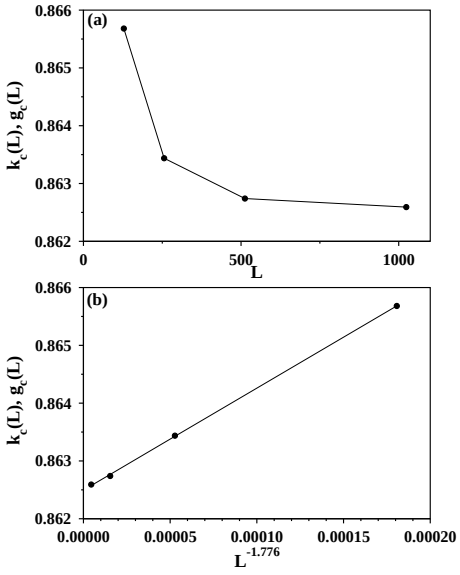


Figure 4: BTW sandpile model: (a) The values of the Kolkata index $k_c(L)$ and the Gini coefficient $g_c(L)$ have been plotted against the system size L for $L = 128$, 256, 512 and 1024. Coefficient values decrease on increasing the system size. (b) The same coefficients have been extrapolated as $L^{-1/\nu}$ where the actual value of ν has been tuned for the best possible linear fit of the data. The plot shows that the best fit corresponds to $1/\nu = 1.776$ which gives $k_c = g_c = 0.863$ in the limit of $L \to \infty$.

four neighboring sites, each grain is transferred to one of the neighboring sites, selected randomly.

$$h(i,j) \to h(i,j) - 2$$
$$h(i_n, j_n) \to h(i_n, j_n) + 1,$$

where (i_n, j_n) is a randomly selected neighboring site and the second equation is executed twice. Using the similar open boundary condition, one finds the average height per site in the stationary state is approximately 0.717157 [14].

2.3. Inequality analysis of the sandpile models

We have studied both the BTW and Manna sandpile models in the subcritical state. Starting from a completely empty lattice, sand grains have been added on to the lattice sequentially one after another. In general, each sand grain addition results an avalanche whose size may be zero or larger. The data for only the non-zero avalanche sizes have been collected till the average height of the sand column per site reaches a pre-assigned value. The total number N of the non-zero avalanches depend on the value of the terminating average height $\langle h(L) \rangle$ where we stop the simulation. In Fig. 2(a) we have plotted this fluctuating sequence of the avalanche sizes s_i as they occur during the sand dropping process, against their serial number i. The avalanche cluster sizes are then sorted out in an ordered increasing sequence $\{s_i, i = 1, N\}$. Further, we have defined a quantity p which is the fraction of avalanches, starting from the smallest to the largest. Simultaneously, we have defined the Lorenz function $L(p) = \Sigma_{i=1}^{i} s_i / \Sigma_{i=1}^{N} s_i$ [1] which represents the fractional cumulative size and its value has been plotted against p (Fig. 2(b)). On this plot both the axes have been normalized to unity. We also draw the $y = 1 - x$ line and the value of the Kolkata index k is obtained by the value of p coordinate of the point of intersection of the $L(p)$ vs. p curve (shown in red) and the $y = 1 - x$ line. In addition, the Gini coefficient g is obtained by doubling the area between the Lorenz curve and the diagonal $y = x$ line.

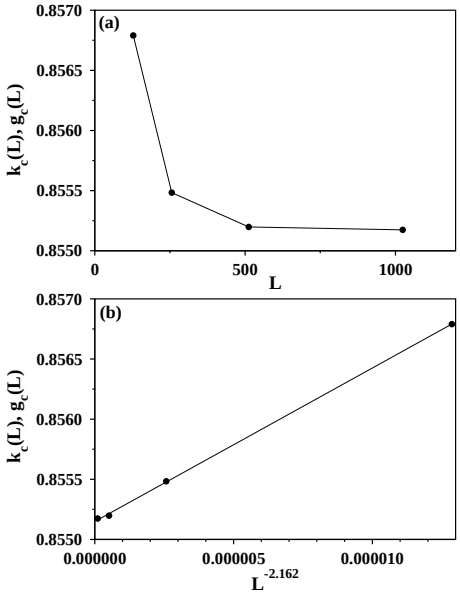


Figure 5: Manna sandpile model: (a) The values of the Kolkata index $k_c(L)$ and the Gini coefficient $g_c(L)$ have been plotted against the system size $L = 128$, 256, 512 and 1024. Coefficient values decrease on increasing the system size. (b) The same coefficients have been extrapolated as $L^{-1/\nu}$ where the actual value of ν has been tuned for the best possible fit of the data. The plot shows that the best fit corresponds to $1/\nu = 2.162$ which give $k_c = g_c = 0.8554$ in the limit of $L \to \infty$.

The values of the Kolkata index (k) and the Gini coefficient (g) have been plotted for the BTW and Manna sandpile models in Fig. 3(a) and Fig. 3(b) respectively. The entire calculation have been done for the four different system sizes, namely, $L = 128$, 256, 512 and 1024; and repeated for 25 values of the terminating average height $\langle h(L)\rangle$ at an interval of 0.002. For every lattice size we have plotted $k(\langle h(L)\rangle, L)$ and $g(\langle h(L)\rangle, L)$ against $\langle h(L)\rangle$. For every lattice size, these two curves intersect at a point which has the coordinates $(\langle h(L)\rangle, k_c(L) = g_c(L))$.

The values of the system size dependent indices are then extrapolated to obtain their asymptotic values in the limit of infinite system size. First, the values of $k_c(L) = g_c(L)$ have been plotted against L in Fig. 4 (a) for the BTW model. In the lower panel Fig. 4(b) the same values have been plotted against $L^{-1/\nu}$ and the value of ν has been tuned so that the data fits best to a linear least square fit. We obtain $1/\nu = 1.776$ and asymptotic values of the indices $k_c = g_c = 0.863$ in the limit of $L \to \infty$. A similar plot in the Fig. 5(a) and Fig. 5(b) for the Manna sandpile yields the best fitted results $1/\nu = 2.162$ and $k_c = g_c = 0.855$ in the limit of $L \to \infty$. A similar method of data analysis had been used to find the asymptotic value of the terminating average height $\langle h(L)\rangle$. In Fig. 6(a) the average heights per site of the BTW model had been extrapolated against $L^{-1.459}$ to obtain the best linear fit. In the limit of $L \to \infty$, we get $h_c = 2.087$. This value is somewhat smaller than the value of the average height 17/8 [13] per site for the BTW model in the limit of $L \to \infty$. Similarly, in Fig. 6(b) we have extrapolated the same data of the Manna sandpile and on extrapolation against $L^{-1.449}$ we obtained $h_c = 0.6859$ to be compared with $h_c \approx 0.717157$ [14].

In Figs. 7(a) and 7(b), k vs g are plotted for the BTW and Manna models respectively. The initial part of the plots fit a straight line, with slopes 0.3876 and 0.3815 in the BTW and Manna models respectively. The plots intersect the $k = g$ line at 0.8628 and 0.8556 for the two models (for system size $L \times L = 512 \times 512$).

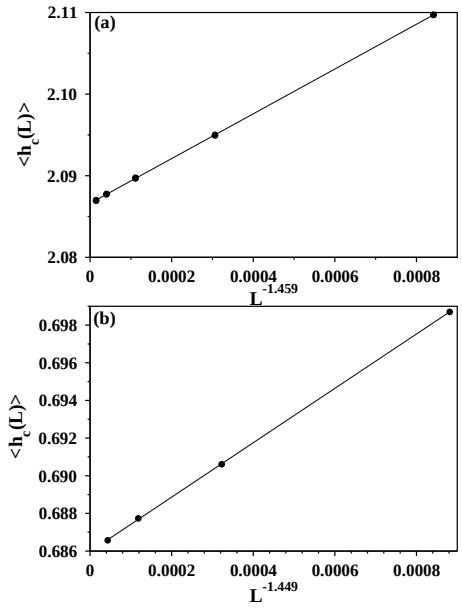


Figure 6: The average height $\langle h_c(L)\rangle$ of the sand column per site corresponding to the point where curves for $k(\langle h\rangle, L)$ and $g(\langle h\rangle, L)$ meet in Fig. 2 have been plotted for $L = 128, 256, 512, 1024$ and 2048. (a) BTW sandpile model: The values of $\langle h_c(L)\rangle$ have been plotted against $L^{-1.459}$ which is extrapolated to $h_c = 2.087$ in the limit of $L \to \infty$. This value is somewhat smaller than the value of the average height 17/8 per site for BTW model with $L \to \infty$ [13]. (b) Manna sandpile model: The values of $\langle h_c(L)\rangle$ have been plotted against $L^{-1.449}$ which is extrapolated to $h_c = 0.6859$ in the limit of $L \to \infty$. This value is somewhat smaller than the value of the average height ≈ 0.717157 per site for Manna model with $L \to \infty$ [14].

3. Inequality measures in the boundary driven Edwards-Wilkinson and centrally loaded fiber bundle models

Quasistatically driven interfaces through a quenched disordered medium can show self-organized critical behavior. Here we analyze two such models, namely the Edwards-Wilkinson mode [11] and the centrally loaded fiber bundle model [12]. Below we first describe the dynamics of these models and then report the inequality measures in the avalanche sizes leading to the critical point.

3.1. Dynamics of the quenched Edwards-Wilkinson model

The Edwards-Wilkinson (EW) model [11] in 1+1 dimension is the simplest model for driven interfaces through random media. For an interface height $h(x,t)$, it reads

$$\frac{\partial h(x,t)}{\partial t} = \nu\nabla^2 h(x,t) + \eta(x,h) + F, \tag{1}$$

where $\eta(x,h)$ is a quenched noise (pinning force) and F is the driving force. The dynamics of the model can be represented in the discrete form as follows $h_i(t+1) = h_i(t) + 1$ if $\tau_i > 0$, where $\tau_i = h_{i+1}(t) + h_{i-1}(t) - 2h_i(t) + \eta_i(h) + F$. The random pinning forces $\eta_i(h)$ are drawn from some probability distribution.

While a depinning tradition can be observed for $F > F_c$, we study here the self-organized critical dynamics of the model, which is driven only at the boundaries [15]. We take a chain of length L and in each stable configuration, move the 0th and $L-1$st points by one unit. There is n other external force anywhere else on the chain. The drive may cause instabilities i.e., other points may move, resulting in an avalanche. The total number of steps moved by all elements until the next stable

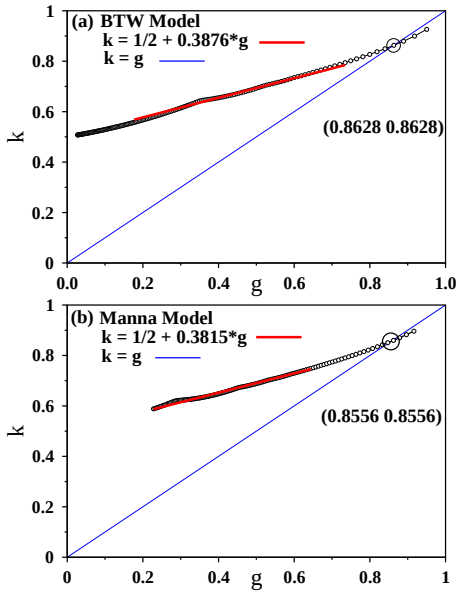


Figure 7: The variations of k versus g in the (a) BTW sandpile model, and (b) Manna sandpile model. The initial parts follow a straight line with slightly different slopes, as indicated in the figures. The crossing points with the $g = k$ line are 0.8628 and 0.8556 respectively.

configuration is reached, is defined as the avalanche size s. Following some transient behavior, the model reaches a self-organized critical state, where the height difference between the end points and the middle point of the chain reaches a stationary value and fluctuates around it. The size distribution of avalanches follow a power law.

3.2. Dynamics of the centrally loaded fiber bundle model

The fiber bundle model [16] is a generic model for failures in disordered materials. For almost a century, the model have been studied by engineers and physicists in the context of catastrophic breakdown processes in driven disordered materials. The centrally loaded fiber bundle model [12], however, does not lead to catastrophic breakdown, but reaches a steady state. The model consists of linear elastic fibers, arranged in a square grid, that are clamped between two plates. The fibers are linear elastic, until the load on it reaches a threshold, beyond which it breaks irreversibly. While the elastic moduli of all fibers are the same, the failure thresholds are in general different and are drawn from a distribution function. The width of the distribution function is a measure of the disorder in the system.

The top plate, from which the fibers are hanging, is rigid, but the bottom plate is very soft. Then a load is applied on a central location, whih is carried by one centrally located fiber. When the load is gradually increased, it crosses the failure threshold of the fiber and the fiber breaks. The load is then carried by it's four nearest neighbors. If that leads to breaking of any one of those neighboring fibers, then the load carried by that fiber is redistributed equally between the surviving neighbors of that broken fiber. For any given load, the centrally located damaged area will continue to increase until a point when all fibers along the damage boundary carry loads that are less than their respective failure thresholds. The load on all fibers along the damage boundary is then increased uniformly until the point when one more fiber breaks and the dynamics is restarted. The numbers of fibers breaking between two successive stable states is the size of the avalanche. Given that the damage boundary, hence the numbers of fibers carrying the applied load will keep

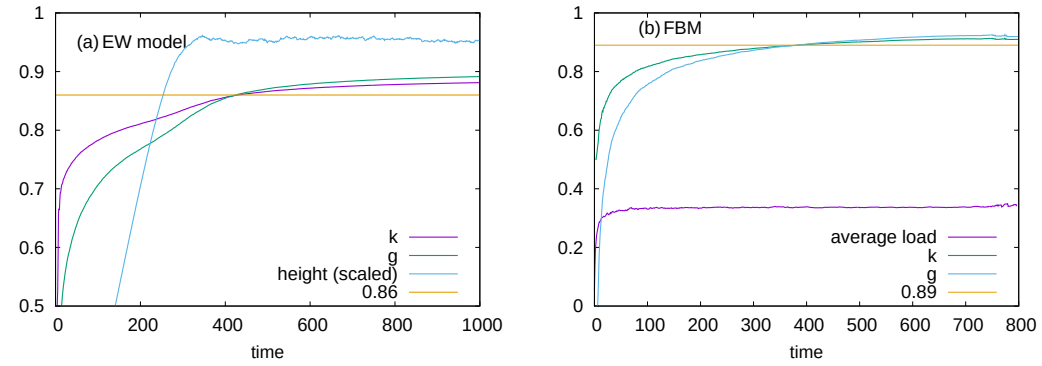


Figure 8: The time variations of k and g indices in the avalanches of the EW and centrally loaded fiber bundle models approaching SOC state. (a) The variations of the k and g indices are shown as functions of time for the EW model. The two indices cross near 0.86. This is close to, but not equal to, the time at which the height difference between the boundary points (where the drive is applied) and the middle point (farthest from the drive) of the EW chain reaches saturation. (b) The same is shown for the centrally loaded fiber bundle model.

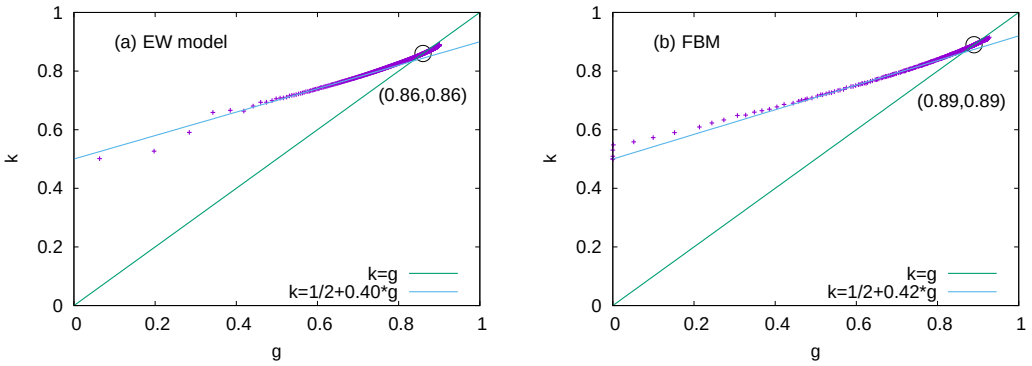


Figure 9: The variations of k versus g in the EW and centrally loaded fiber bundle models. (a) The variations of k versus g indices are shown for the EW model. The initial slope of the k versus g plot is 0.40. (b) The same is plotted for the centrally loaded fiber bundle model. The slope here is 0.42.

on increasing, the model will never show catastrophic breakdown in the thermodynamic limit. It turns out that the average load per fiber reaches a value 1/3, if the threshold distribution is uniform in (0,1). This is a self-organized critical point and the avalanche sizes show a power law distribution with exponent value $-3/2$ [12].

Here we look at the avalanches, starting from the breaking of the first centrally located fiber, as the system reaches the self-organized critical point and measure inequalities in the avalanche sizes.

3.3. Inequality analysis of the interface models

In Fig. 8(a), the averaged values of g, k and the height difference between the boundary points and the middle point scaled by a factor, are shown for uniform distributions of the pinning forces in (0,2) in the EW model. The crossing points of g and k are surprisingly close to 0.86. The same observation is found for triangular and Gaussian distributions of the pinning forces (not shown). In Fig. 8(b), we plot the same for the centrally loaded fiber bundle model. The crossing point in this case is slightly higher (0.89).

In Fig. 9(a) k versus g is plotted for the EW model. The initial part is linear, with a slope 0.40. In Fig. 9(b) the same is plotted for the centrally loaded fiber bundle model. In this case, the initial linear slope is 0.42.

Other than the surprisingly close values of the crossing points of g and k in the various different models, the linear variation with a near-universal slope in k versus g plots seems to be rather crucial. Indeed, in the rel data for diverse socioeconomic systems, such behavior have been already observed [7]. This is particularly important in view of the fact that many socioeconomic systems with unrestricted competition are assumed to be in an SOC state.

4. Discussions and conclusions

In socio-economic systems with unrestricted competitions, emergence of inequality in resource distributions is observed very often [7, 17]. Such inequalities are quantified using some indices, related to the distributions of the individual resources through the Lorenz function $L(p)$. Here we have studied the Gini index g (given by the ratio of the area between the equality line and the Lorenz curve and the area under the equality line), and the Kolkata index k (given by the fixed point of the complementary Lorenz function $\tilde{L}(p) \equiv 1 - L(p)$), giving the magnitude of the fraction k of resource possessed by the fraction $1 - k$ of the population (see Fig. 1). It was seen before that $g_c = k_c \approx 0.87$ in systems with unrestricted competitions (see e.g., [7, 17]).

We have shown here, through numerical analysis, that the same behavior are shown by four self-organized critical models, namely the BTW sandile [9], Manna sandpile [10], quenched EW model [11] and the centrally loaded fiber bundle model [12], in their course towards the respective self-organized critical points. Particularly, from the time series of the avalanches in these models, we first construct the Lorenz curve (see Fig. 1). Then from its fixed point the inequality index k is estimated and from the area between the equality line and the Lorenz curve the value of g is estimated. The Lorenz curve is discrete here and the corresponding error bars in g and k depends upon the point spacings, which in turn depend upon the system size. Finite size scaling reveals that the crossing points of g and k as functions of the average sandpile height differ only slightly (less than 3%) from the respective critical heights. Specifically, for the BTW model, the crossing point for k and g is at $k_c = g_c = 0.863$ (Fig. 3) when extrapolated to $L \to \infty$ while the average height of the BTW sandpile at that point is 2.087 (Fig. 5), which is slightly less than the critical height [13] of the BTW sandpile (17/8). For the Manna sandpile model, the crossing point of k and g is at $k_c = g_c = 0.8554$ (Fig. 4) The average sandpile height at that point is 0.6859 (Fig. 5), while the critical height is at 0.717157 [14] for the Manna model. Also, the slope of the k versus g line at

the initial stage (prior to reaching SOC state) is 0.3876 and 0.3815 for the BTW and Manna model (Fig. 7) respectively. In the EW interface, the crossing point of k versus g is $k_c = g_c \simeq 0.86$ and that for the centrally loaded fiber bundle model is about 0.89 (Fig. 8). The initial linear part of the k versus g plots have slope 0.40 and 0.42 respectively for the EW and the centrally loaded FBM (Fig. 9). A comparison with similar observations in socio-economic data (see e.g., [17]) suggests similar emergent inequality as a result of unconstrained competitions in the social dynamics.

The underlying physical origin of this numerical observation, seen here in SOC models of distinct universality classes, and also seen elsewhere in socio-economic systems [7, 17] presumably operating in SOC points, is an important open question. While some recent progresses have been made in analytically (see e.g., [18]), further extensive analysis both in models and data (e.g., see [19]) are needed.

In conclusions, the self-organized critical (SOC) models we studied here show near universal characteristics in terms of the inequality measures of their 'avalanche' statistics in their respective approach to the SOC points. This stands as a quantitative support the existence of SOC behavior in socio-economic systems. Such observations can also help in estimating the 'distance' from the imminent disaster or SOC points for those complex systems for which such model studies are not possible.

Acknowledgement: SSM is thankful to S. N. Bose National Centre for Basic Sciences, Kolkata for the support through the Visiting (Honorary) Fellow position. BKC is grateful to the Indian National Science Academy for their support through the Senior Scientist Research Grant.

References

[1] M. O. Lorenz, *Methods of measuring the concentration of wealth*, Publication of the American Statistical Association **9**, 209219 (1905).

[2] C. Gini, Measurement of inequality of incomes. Economics Journal **31**, 124126 (1921)

[3] A. Ghosh, N. Chattopadhyay and B. K. Chakrabarti, *Inequality in societies, academic institutions and science journals: Gini and k-indices*, Physica A: Statistical Mechanics and Applications **410**, 3034 (2014).

[4] S. Banerjee, B. K. Chakrabarti, M. Mitra, and S. Mutuswami, *Inequality measures: The kolkata index in comparison with other measures*, Frontiers in Physics **8**, 562182 (2020)

[5] V. Pareto, A. N. Page, *Translation of 'Manuale di economia politica' (Manual of political economy)*, A.M. Kelley Publishing, New York (1971)

[6] A. Chatterjee, A. Ghosh, and B. K. Chakrabarti, *Socio-economic inequality: Relationship between Gini and Kolkata indices*, Physica A: Statistical Mechanics and its Applications **466**, 583 (2017)

[7] A. Ghosh and B. K. Chakrabarti, *Limiting value of the Kolkata index for social inequality and a possible social constant*, Physica A: Statistical Mechanics and its Application **573**, 125944 (2021)

[8] S. Biswas and B. K. Chakrabarti, *Social inequality analysis of fiber bundle model statistics and prediction of materials failure*, Phys. Rev. E **104**, 044308 (2021)

[9] P. Bak, C. Tang and K. Wiesenfeld, *Self-organized criticality: an explanation of* $1/f$ *noise*, Phys. Rev. Lett. **59**, 381 (1987).

[10] S. S. Manna, *Two-state model of self-organized criticality*, J. Phys. A: Math. Gen. **24**, L363 (1991).

[11] S. F. Edwards, D. R. Wilkinson, *The surface statistics of a granular aggregate*, Proc. R. Soc. Lond. A **381**, 17 (1982).

[12] S. Biswas, B. K. Chakrabarti, *Self-organized dynamics in local load-sharing fiber bundle models*, Phys. Rev. E **88**, 042112 (2013).

[13] L. Levine and Y. Peres, *The looping constant of* Z^d, Random Structures & Algorithms **45**, 1 (2014).

[14] S. S. Manna, unpublished result (2021).

[15] S. Biswas, P. Ray, B. K. Chakrabarti, *Equivalence of the train model of earthquake and boundary driven Edwards-Wilkinson interface*, Eur. Phys. J. B **86**, 388 (2013).

[16] S. Pradhan, A. Hansen, B. K. Chakrabarti, *Failure processes in elastic fiber bundles*, Rev. Mod. Phys **82**, 499 (2010).

[17] S. Banerjee, S. Biswas, B. K. Chakrabarti, A. Ghosh, R. Maiti, M. Mitra, D. R. S. Ram, *Evolutionary Dynamics of Social Inequality and Coincidence of Gini and Kolkata indices under Unrestricted Competition*, arXiv:2111.07516 (2021).

[18] B. Joseph, B. K. Chakrabarti, *Variation of Gini and Kolkata Indices with Saving Propensity in the Kinetic Exchange Model of Wealth Distribution: An Analytical Study* , Physica A (in press) arXiv:2110.15001 (2021).

[19] M. Jusup, P. Holme, K. Kanazawa, M. Takayasu, I. Romic, Z. Wang, S. Gecek, T. Lipic, B. Podobnik, L. Wang, W. Luo, T. Klanjscek, J. Fan, S. Boccaletti, M. Perc, *Social physics*, Phys. Rep. **948**, 1-148 (2022).